

## Stark Spectroscopic Studies of Blue Copper Proteins: Azurin

Arindam Chowdhury and Linda A. Peteanu\*

Department of Chemistry, Carnegie Mellon University, Pittsburgh, Pennsylvania 15213

M. Adam Webb and Glen R. Loppnow

Department of Chemistry, University of Alberta, Edmonton, Alberta, Canada T6G 2G2

Received: July 18, 2000; In Final Form: October 5, 2000

The change in the dipole moments ( $|\overline{\Delta\mu}|$ ) and the average change in the polarizability ( $\langle\overline{\Delta\alpha}\rangle$ ) upon excitation for the Cys(S) $\rightarrow$ Cu(II) ligand-to-metal charge-transfer (LMCT) transitions in two species of azurin, a type I blue copper protein from *Alcaligenes denitrificans* (AD) and *Pseudomonas aeruginosa* (PA), were determined using Stark (electroabsorption) spectroscopy. Measurements at 77 K in a glycerol-water glassy matrix yield a value for  $|\overline{\Delta\mu}|$  of between 1.3 and 2.0 D. This value of  $|\overline{\Delta\mu}|$  is consistent with the highly covalent nature of the S–Cu bond in the ground state and is in agreement with the predictions of previous electronic structure calculations. The polarizability of the excited state was smaller than the ground state by about 10–20 Å<sup>3</sup>. This negative value of  $\langle\overline{\Delta\alpha}\rangle$ , which is somewhat unusual, is interpreted in the context of the two-state model. Values for the electron-transfer matrix element ( $H_{ab}$ ) and the effective charge-transfer distance ( $R_{ab}$ ) derived from our measurements are also reported.

## Introduction

Blue copper proteins are involved in respiratory and photosynthetic electron transport.<sup>1–3</sup> Azurin, a 14.6-kDa type I copper protein (“cupredoxin”), is found in denitrifying bacteria and is thought to play a role in denitrification and the mediation of cellular responses to redox stress. Type I cupredoxins are characterized by an intense ( $\epsilon = 2000\text{--}6000\text{ cm}^{-1}\text{ M}^{-1}$ ) charge-transfer absorption band at  $\sim 600\text{ nm}$ , narrow hyperfine splitting ( $A_{\parallel} = 35\text{--}63 \times 10^{-4}\text{ cm}^{-1}$ ) in the  $g_{\parallel}$  region, and copper(II) reduction potentials that range from 184 to 680 mV, significantly higher than that of aqueous copper(II) at 115 mV.<sup>2,3</sup> These unusual electronic properties are thought to arise from the unique coordination geometry imposed on the copper site by the protein. The structure of azurin shows a copper ion in an elongated, distorted trigonal bipyramidal coordination environment, with His46, Cys 112, and His117 as the three strongly bound planar ligands, and Met121 and the carbonyl oxygen of Gly45 as the two weakly bound axial ligands (Figure 1).<sup>2</sup>

Several techniques have been used to correlate electronic structure and coordination geometry with observed electron-transfer rates and driving forces (redox potential). The electronic structure of azurin has been studied extensively with low-temperature absorption, circular dichroism (CD), and magnetic circular dichroism (MCD) spectroscopy.<sup>4–7</sup> In addition, spectroscopic and self-consistent-field X $\alpha$ -scattered wave (SCF-X $\alpha$ -SW) studies of plastocyanin, a type I cupredoxin, which has been suggested to have an electronic structure similar to azurin, have also been performed.<sup>8,9</sup> Site-directed mutagenesis followed by complexation with exogenous ligands has been used to examine the role of the axial ligands in determining the electronic structure of blue copper proteins.<sup>10,11</sup> All of these studies suggest that the most intense band in the visible absorption spectrum is a nominal S(Cys- $\pi$ ) $\rightarrow$ Cu ligand-to-metal charge transfer (LMCT) transition. Weaker transitions at higher energy are S(Cys- $\sigma$ ) $\rightarrow$ Cu, S(Met- $\sigma$ ) $\rightarrow$ Cu, and N(His- $\pi$ ) $\rightarrow$ Cu

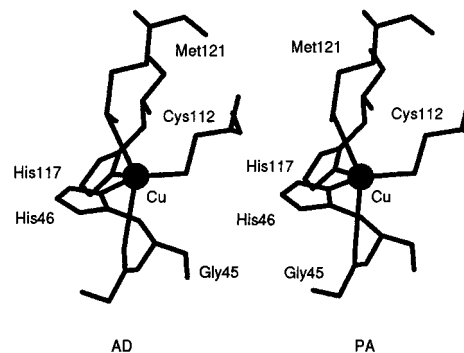
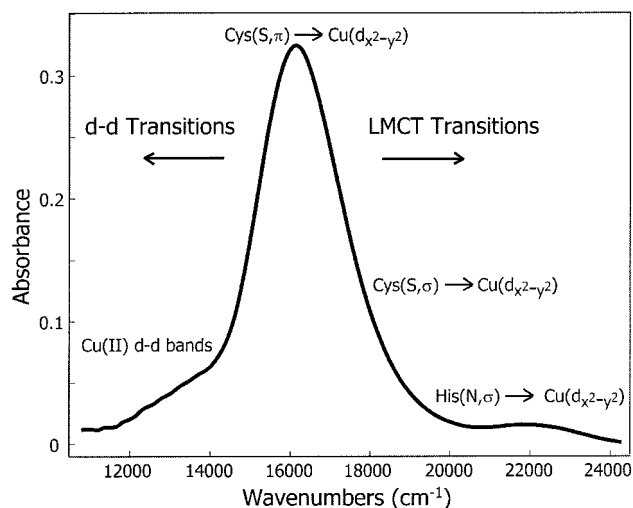


Figure 1. Active site of AD and PA azurin.

charge-transfer transitions, whereas the weaker transitions at lower energy are primarily ligand-field transitions (Figure 2). The axial ligand (Met121) appears to play a substantial role in tuning the electronic properties of the copper site, but is not necessary for the formation of a blue copper site. X-ray absorption spectroscopy has shown that the Cu-S<sub>Cys</sub> bond in plastocyanin is unusually covalent and it has been suggested that it provides a preferred pathway for biological ground-state electron transfer.<sup>9</sup>

Electroabsorption (Stark) spectroscopy has been applied to the study of intramolecular electron transfer in several organic, inorganic, and biological systems. For some examples of applications to inorganic systems and a recent review, see refs 12–16. The method involves applying an external field on the sample and monitoring the consequent shift and broadening of the absorption band induced by the field. Analysis of the field-induced perturbation of the absorption spectrum of an isotropic sample allows both the absolute value of the change in dipole moment,  $\overline{\Delta\mu}$  ( $|\overline{\Delta\mu}|$ ), and the average change in the polariz-



**Figure 2.** Charge-transfer transitions within the absorption band of PA azurin. Assignments shown are from adapted from ref 6.

ability ( $\langle \Delta\alpha \rangle$ , where the bar underneath denotes that it is a tensor quantity) between the lower and upper states of the optical transition to be discerned. Occasionally, field-induced changes in the transition moment of the molecule are observed as well. The value of  $|\Delta\mu|$  is directly correlated to the change in the extent of charge transfer in the excited state, relative to that in the ground state. This is typically the quantity of interest also in the study of optical charge-transfer and electron-transfer systems. The interpretation of  $\langle \Delta\alpha \rangle$  is somewhat more complex, because this quantity reflects the interactions between the electronic states being probed and all other electronic states of the system. It is also often regarded as a measure of the change in the extent of electron delocalization upon optical excitation.

Stark spectroscopy provides information regarding the fundamental properties of the electronic states of the blue copper protein systems, in the form of  $|\Delta\mu|$  and  $\langle \Delta\alpha \rangle$ , that complements spectroscopic and electronic structure studies currently in the literature. Moreover, these quantities provide critical input to another important class of experiments, those that probe the photoinduced charge-transfer process using time-resolved optical techniques,<sup>17,18</sup> and to the associated theoretical models of the protein response<sup>19</sup> described below.

Interest in elucidating the role of the protein in determining the rate, efficiency, and pathways of biological electron transfer has prompted a considerable effort in studying *excited state* charge transfer (CT) that is initiated by absorption of a photon. One interesting aspect of the electron-transfer process that can be probed readily using optical techniques is the contribution of the protein to the electron-transfer reorganization energy. Toward this goal, the response of the protein plastocyanin to the change in charge distribution from the ground to the excited state has been followed by monitoring the transient absorption signal following excitation either into the *d-d* transitions<sup>17</sup> or into the main CT band.<sup>18</sup> The resulting spectral evolution presumably contains contributions both due to protein 'solvation' of the excited-state charge distribution and from population relaxation within the complex electronic manifold of the system. However, the measured  $\Delta\mu$  for excitation into the charge-transfer band allows the contribution to the ultrafast dynamics that is due to dielectric relaxation of the protein to be modeled accurately.

Here we report the results of electroabsorption spectroscopy on the most intense LMCT transition for azurin from *Alcaligenes denitrificans* (AD) and *Pseudomonas aeruginosa* (PA). Azurin

was chosen for our initial studies because the visible absorption band is dominated by a single charge-transfer transition.<sup>6</sup> This minimizes a complication that sometimes arises in the analysis of electroabsorption spectra, specifically the presence of multiple closely spaced electronic states having varying responses to the applied field.<sup>20,21</sup> The results presented here demonstrate that the value of  $|\Delta\mu|$  for the main charge-transfer band of both azurins is small, in agreement with electronic structure calculations<sup>22–25</sup> and X-ray absorption studies<sup>9,26,27</sup> of blue copper systems. In addition, we report a *negative* value for  $\langle \Delta\alpha \rangle$  and discuss this unusual finding in the context of previously published results from time-resolved measurements on the related blue copper protein plastocyanin. Stark spectroscopic studies of plastocyanin are currently in progress.<sup>28</sup>

## Experimental

**Sample Isolation and Preparation.** Preparation of azurin from PA was based on a modification of literature procedures<sup>29–31</sup> and has been reported previously.<sup>32</sup> Purity ratios ( $A_{280}/A_{625}$ ) obtained were less than 2.1, close to the reported value of 1.7. A yield of 13–56 mg PA azurin per 100 g cell paste was obtained using this method. The yield of azurin was found to be greatly dependent on the growth conditions of the bacteria; the yield was greatly reduced when the cells were overgrown.

Azurin from AD was isolated and purified using a method developed for *Alcaligenes xylosoxidans*. This protocol seemed to yield a purer, higher yield of protein than previously reported procedures. Azurin was purified using reported methods<sup>30,33,34</sup> with slight modifications in the cell rupture and column chromatography steps. The extraction was similar to what was mentioned above using 0.02 M ammonium acetate, pH 6.0. A two-step ammonium sulfate precipitation was performed at 30% and 100% w/v, and the resulting pellet was dissolved in a minimal amount of water and adjusted to pH 7.0 before dialysis against water. Column chromatography was performed using Whatman CM-52 {no Na[Co(EDTA)]} and Sephadex G-50 {with Na[Co(EDTA)]} columns until the purity ratio ( $A_{280}/A_{620}$ ) for azurin was  $\leq 3.8$ , close to the literature value of 3.6. Typical yields were 46–58 mg AD azurin per 100 g of cell paste.

**Theory of Electroabsorption and Data Analysis Procedures.** The analysis of the electroabsorption data is similar to what has been reported.<sup>14,35</sup> The equations shown here are appropriate for the experimental conditions used, that is, the sample is embedded isotropically in a rigid glass. Essentially, the change in absorption due to the application of an external electric field is fit to the weighted sum of zeroth, first and second derivatives of the zero-field absorption spectrum. The overall change in absorbance caused by the application of an electric field is described by the following equation:

$$\Delta A(\tilde{\nu}) = \bar{\mathbf{F}}_{\text{eff}}^2 \left[ \mathbf{a}_{\chi} A(\tilde{\nu}) + \mathbf{b}_{\chi} \frac{\tilde{\nu}}{15\hbar} \left\{ \frac{\partial}{\partial \tilde{\nu}} \left( \frac{A(\tilde{\nu})}{\tilde{\nu}} \right) \right\} + \mathbf{c}_{\chi} \frac{\tilde{\nu}}{30\hbar^2} \left\{ \frac{\partial^2}{\partial \tilde{\nu}^2} \left( \frac{A(\tilde{\nu})}{\tilde{\nu}} \right) \right\} \right] \quad (1)$$

The  $A(\tilde{\nu})$  represents the unperturbed absorption as a function of frequency ( $\tilde{\nu}$ ) and  $\bar{\mathbf{F}}_{\text{eff}}$  represents the field at the sample in volts per centimeter. This effective field includes the enhancement of the applied field due to the cavity field of the matrix. The subscript  $\chi$  represents the angle between the direction of the applied electric field and the electric field vector of the polarized light. The expressions for  $\mathbf{a}_{\chi}$ ,  $\mathbf{b}_{\chi}$ , and  $\mathbf{c}_{\chi}$  are given below:

$$\mathbf{a}_\chi = \frac{1}{30|\bar{m}|^2} \sum_{ij} [10A_{ij}^2 + (3A_{ii}A_{jj} + 3A_{ij}A_{ji} - 2A_{ij}^2) \cdot (3 \cos^2\chi - 1)] + \frac{1}{15|\bar{m}|^2} \sum_{ij} [10m_i B_{ijj} + (3m_i B_{jij} + 3m_i B_{jji} - 2m_i B_{ijj}) \cdot (3 \cos^2\chi - 1)] \quad (2)$$

$$\mathbf{b}_\chi = \frac{1}{|\bar{m}|^2} \sum_{ij} [10m_i A_{ij} \Delta\mu_j + (3m_i A_{ji} \Delta\mu_j + 3m_i A_{jj} \Delta\mu_i - 2m_i A_{ij} \Delta\mu_j) \cdot (3 \cos^2\chi - 1)] + \frac{15}{2} \langle \Delta\alpha \rangle + \frac{3}{2} [\Delta\alpha_m - \langle \Delta\alpha \rangle] \cdot (3 \cos^2\chi - 1) \quad (3)$$

$$\mathbf{c}_\chi = 5|\bar{\Delta\mu}|^2 + |\bar{\Delta\mu}|^2 \cdot [(3 \cos^2\xi - 1) \cdot (3 \cos^2\chi - 1)] \quad (4)$$

Here,  $\xi$  is the angle between  $\bar{\Delta\mu}$  and  $\bar{m}$ , the transition moment vector. In each case, if the experiment is performed at the magic angle ( $\chi = 54.7^\circ$ ) the expressions are simplified because  $(3 \cos^2\chi - 1)$  is equal to zero.

In this work we quote  $\langle \Delta\alpha \rangle$ , which represents the average change in electronic polarizability between the ground and excited state [i.e.,  $\langle \Delta\alpha \rangle = 1/3 \text{Tr}(\Delta\alpha)$ ] and  $\Delta\alpha_m$  is its projection along the transition moment direction. The tensors  $\underline{A}$  and  $\underline{B}$  represent the transition polarizability and hyperpolarizability, respectively. These describe the effect of  $\bar{\mathbf{F}}_{\text{eff}}$  on the molecular transition moment:  $\bar{m}(\bar{\mathbf{F}}_{\text{eff}}) = \bar{m} + \underline{A} \cdot \bar{\mathbf{F}}_{\text{eff}} + \bar{\mathbf{F}}_{\text{eff}} \cdot \underline{B} \cdot \bar{\mathbf{F}}_{\text{eff}}$ . Generally, this term can be neglected for strongly allowed transitions. Moreover, for a small  $|\Delta\mu|$ , such as is measured here for the azurins (see Results), the cross-terms involving the elements of the tensor  $\underline{A}$  can be neglected compared with the other terms in the expression for  $\langle \Delta\alpha \rangle$  (eq 3).

Information regarding  $|\Delta\mu|$  for the molecule is contained in the  $c_\chi$  term (eq 4). For an isotropic sample such as those studied in this work, only the magnitude and not the sign of  $\Delta\mu$  is measured. For a more detailed discussion of these effects, see refs 14 and 35.

The experiment is normally performed at two angles,  $\chi = 54.7^\circ$  (magic angle) and  $\chi = 90^\circ$ . The utility of the measurements at  $\chi = 90^\circ$  and  $\chi = 54.7^\circ$  in the context of the results presented here is as follows. At  $\chi = 90^\circ$  and  $\chi = 54.7^\circ$ , the coefficients  $c_\chi$  are reduced to:

$$\mathbf{c}_{90} = 5|\bar{\Delta\mu}|^2 - |\bar{\Delta\mu}|^2 \cdot (3 \cos^2\chi - 1) \quad (5)$$

$$\mathbf{c}_{54.7} = 5|\bar{\Delta\mu}|^2 \quad (6)$$

The expression for  $\mathbf{c}_{90}$  is reduced to eq 7 for  $\xi = 0$ ,

$$\mathbf{c}_{90} = 3|\bar{\Delta\mu}|^2 \quad \text{if } \xi = 0, \text{ i.e. if } \bar{\Delta\mu} \text{ parallel to } \bar{m} \quad (7)$$

Similarly, at  $\chi = 90^\circ$  and  $\chi = 54.7^\circ$ , the coefficients  $\mathbf{b}_\chi$  are reduced to:

$$\mathbf{b}_{90} = \frac{3}{|\bar{m}|^2} \sum_{ij} [4m_i A_{ij} \Delta\mu_j - m_i A_{ji} \Delta\mu_j - m_i A_{jj} \Delta\mu_i] + \frac{15}{2} \langle \Delta\alpha \rangle + \frac{3}{2} [(\Delta\alpha) - \Delta\alpha_m] \quad (8)$$

$$\mathbf{b}_{54.7} = \frac{10}{|\bar{m}|^2} \sum_{ij} m_i A_{ij} \Delta\mu_j + \frac{15}{2} \langle \Delta\alpha \rangle \quad (9)$$

In the expressions for  $\mathbf{b}_{90}$  and  $\mathbf{b}_{54.7}$  (eqs 8 and 9), the terms containing the transition moment polarizability tensor,  $\underline{A}$ , can be neglected because they are expected to be small compared with the other terms (see below). Hence the expressions for  $\mathbf{b}_{90}$  and  $\mathbf{b}_{54.7}$  are reduced to the form:

$$\mathbf{b}_{90} \approx \frac{15}{2} \langle \Delta\alpha \rangle + \frac{3}{2} [(\Delta\alpha) - \Delta\alpha_m] \quad (10)$$

$$\mathbf{b}_{54.7} \approx \frac{15}{2} \langle \Delta\alpha \rangle \quad (11)$$

It can be shown that if  $\Delta\alpha_m = \text{Tr}(\Delta\alpha)$  (i.e., only the components of  $\Delta\alpha$  along the transition moment direction are nonzero),  $\mathbf{b}_{90}$  is reduced to the form shown in eq 12.

$$\mathbf{b}_{90} \approx \frac{9}{2} \langle \Delta\alpha \rangle \quad \text{if } \Delta\alpha_m \approx \text{Tr}(\Delta\alpha) = 3 \langle \Delta\alpha \rangle \quad (12)$$

Under these circumstances, the ratios of both  $\mathbf{b}_\chi$  and  $\mathbf{c}_\chi$  at  $54.7^\circ$  versus  $90^\circ$  (using eqs 6, 7, 11, and 12) are equal to 1.667. Therefore, we have reported this ratio for the two azurins (Results section) studied here to show that, for the main charge-transfer transition,  $\Delta\mu$  is parallel to the direction of the transition moment and that the only nonzero components of  $\Delta\alpha$  are those along the transition moment, within our experimental error.

The coefficients,  $\mathbf{a}_\chi$ ,  $\mathbf{b}_\chi$ , and  $\mathbf{c}_\chi$ , are extracted by means of a linear least-squares (LLSQ) fit of the electroabsorption signal to the sum of the derivatives of  $A(\tilde{\nu})$ . If the resultant fit to the absorption line shape (a single set of  $\mathbf{a}_\chi$ ,  $\mathbf{b}_\chi$ , and  $\mathbf{c}_\chi$ ) is not of high quality, this indicates that there is more than one transition (electronic or vibronic) underlying the absorption band, each of which has different electrooptical properties ( $|\Delta\mu|$  and/or  $\langle \Delta\alpha \rangle$ ). This is the case for the electroabsorption spectra of both PA and AD azurin presented here. In such instances, the fit to the electroabsorption spectrum can be improved by modeling the underlying transitions in the absorption band as Gaussians. To implement this method, it is helpful to have independent data regarding the number, positions, and widths of the electronic transitions underlying the absorption band. These data allow the properties of the Gaussians representing the individual transitions to be constrained so as to minimize the number of free parameters in the fitting.

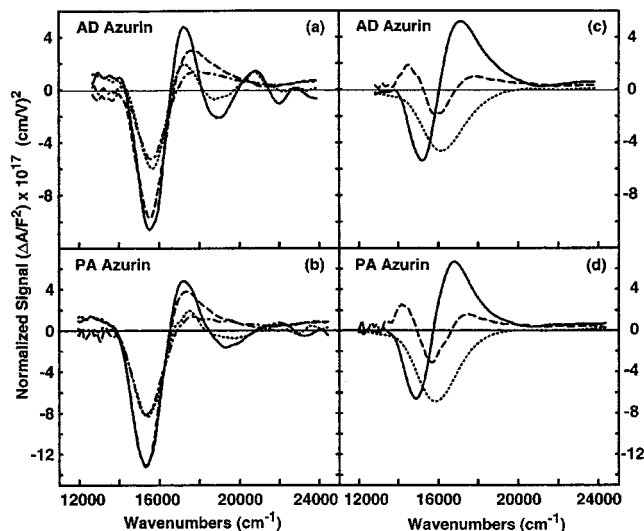
The starting parameters for the bands used to fit the absorption spectra of PA azurin were chosen using, as a guide, the MCD data by Solomon et al.<sup>6</sup> for PA azurin at 35 K. Those for AD azurin were generated by shifting the positions of each Gaussian by  $\sim 310 \text{ cm}^{-1}$  to account for the difference in the absorption maxima between the two proteins. These initial parameters were varied using a simplex routine to obtain the best fit to the PA and AD azurin absorption spectra. The final parameters for all Gaussians are summarized in Table 1.<sup>36</sup> Values of  $\mathbf{a}_\chi$ ,  $\mathbf{b}_\chi$ , and  $\mathbf{c}_\chi$  for each Gaussian were then found through the fitting process. Using these coefficients and eqs 2–4 above, a value of  $|\Delta\mu|$  and  $\langle \Delta\alpha \rangle$  was assigned to each transition. We have used this method previously, and it is explained in detail in ref 21.

## Results

Figure 3 contains the electroabsorption spectra of both PA and AD azurins obtained at  $\chi = 90^\circ$  and  $54.7^\circ$  (solid lines, Figures 3a and 3b, respectively). Overall, the absorption and electroabsorption spectra of the two species are similar in appearance. Likewise, both proteins exhibit a response to the applied field (total signal) that is similar in magnitude. The fits

**TABLE 1: Parameters of the Gaussians Used to Model the Absorption Spectra of AD and PA Azurin in Glycerol/Buffer Glass at 77 K**

Gaussians	AD azurin				PA azurin			
	I	II	III	IV	I	II	III	IV
center <sup>a</sup>	13215	16148	18239	21793	12975	15865	17800	20500
relative height	0.1331	1.0	0.1608	0.0499	0.0787	1.0	0.1241	0.037
half-width at half-maximum <sup>a</sup>	970	994	975	1320	700	935	900	1200

<sup>a</sup> Reported in cm<sup>-1</sup>.

**Figure 3.** Electroabsorption spectra and the fit to the electroabsorption signal for both AD (a) and PA (b) azurins are shown as a function of the angle  $\chi$  (see Experimental Section). For both the azurins, the electroabsorption signal normalized with the square of the applied field at  $\chi = 90^\circ$  (dotted lines) and  $\chi = 54.7^\circ$  (solid lines) and the fit to the electroabsorption signal at  $\chi = 90^\circ$  (dashed-dot lines) and  $\chi = 54.7^\circ$  (dashed lines) are shown. The zeroth derivative (dotted lines), first derivative (solid lines), and the second derivative (dashed lines) components of the absorption spectrum at  $\chi = 54.7^\circ$ , normalized with respect to the square of the applied field for AD (c) and PA (d) azurins are shown.

to these spectra, obtained from taking derivatives of the experimental absorption spectra (dashed lines), are also shown in the figure. These fits are then decomposed into their respective zeroth, first, and second derivative contributions that are shown in Figures 3c and 3d. To improve the quality of the fits to the electroabsorption spectra, two additional fitting strategies were used (shown in Figure 4). This figure contains fits to the electroabsorption spectra at  $\chi = 54.7^\circ$  that were obtained by truncating the experimental absorption bands (Figures 4c and 4g) and by using Gaussians (Figures 4d and 4h) to model the absorption bands. The details of the procedures used to produce these fits are described below.

Because the absorption spectra of both species are dominated by a single CT transition, the Cys(S- $\pi$ ) $\rightarrow$ Cu (II) LMCT band, we initially modeled their electroabsorption spectra using weighted derivatives of their respective absorption spectra over the full wavenumber range ( $\sim 11\,000$ – $24\,000$  cm<sup>-1</sup>), as described in the Experimental section. The resulting fits are shown as the dashed lines in Figures 4b and 4f. Although the quality of the fits to the largest feature of both electroabsorption spectra is quite reasonable, deviations are seen in the higher-energy portions of the spectra. These deviations are most likely due to the presence of weaker CT transitions that lie within the main absorption band of both AD and PA. If these transitions have values of  $|\Delta\mu|$  and/or  $\langle\Delta\alpha\rangle$  that are significantly different from those of the main CT band, they will exhibit a measurably different response to the applied field. Below we describe two

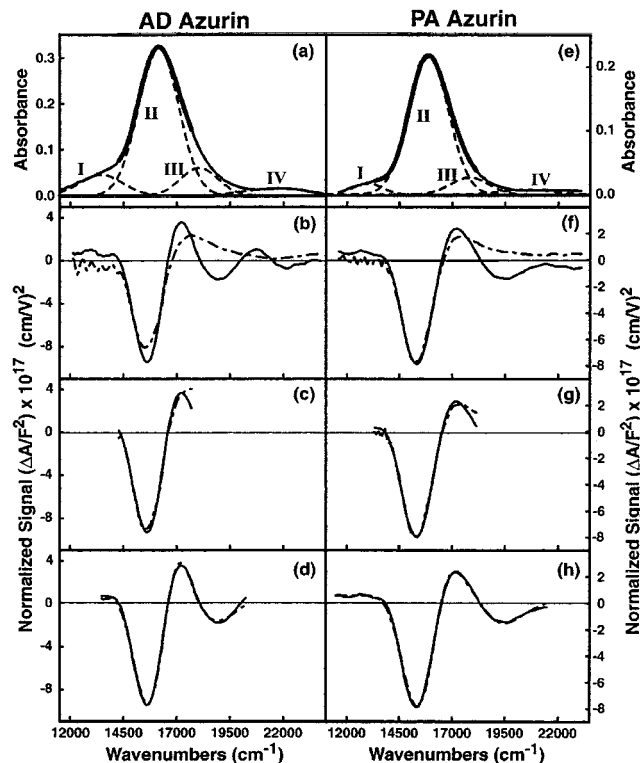


**Figure 4.** Absorption and electroabsorption spectra of AD and PA azurins. Panels a and e contain the absorption spectra of AD and PA azurins in which the Gaussians used to deconvolve the spectrum are designated as I–IV (see Experimental section). Panels b and f contain the experimental electroabsorption spectra normalized by the square of the applied electric field (solid line) and the fits to these spectra (dashed lines) obtained using eqs 1–4 (see text) and a single set of electrooptical parameters ( $\mathbf{a}_\chi$ ,  $\mathbf{b}_\chi$ ,  $\mathbf{c}_\chi$ ). Panels c and g show the results of fitting the central band of the normalized electroabsorption spectra of AD and PA azurins to the segment of the absorption spectra shown in dark pen in panels a and e, respectively. Panels d and h show the fits to the normalized electroabsorption spectra obtained using Gaussians II and III as described in the text.

methods to account for such heterogeneity in the absorption bands which can be used to improve the fits to the electroabsorption spectra presented here.

One method to extract the properties of the predominant CT transition of the azurins is to fit only the most intense region of their electroabsorption spectra using the portion of their absorption spectra that lies within the same wavenumber region. By this means, the contributions of the weaker  $d-d$  and CT bands to the fit are effectively minimized. This fitting method yielded reliable results if the transitions underlying the absorption band are not overlapped too strongly or if, as is the case here, a single transition dominates the spectrum. The segments of the absorption spectra used here are depicted in heavy pen in Figures 4a and 4e. The resulting fits to the main feature of the electroabsorption spectra of AD and PA azurin are shown in Figures 4c and 4g, respectively. For AD azurin, the resulting fit in the most intense region of the electroabsorption spectrum is substantially

**TABLE 2: Electroabsorption Results for the Cys-S( $\pi$ ) $\rightarrow$ Cu(II) Transition of AD and PA Azurin in Glycerol/Buffer Glass at 77 K**

Azurin	Truncated absorption spectrum		Gaussians to fit the absorption spectrum	
	$ \overline{\Delta\mu} ^a$	$\langle\overline{\Delta\alpha}\rangle^b$	$ \overline{\Delta\mu} ^a$	$\langle\overline{\Delta\alpha}\rangle^b$
<i>A. deinitrificans</i>	1.4 (0.1)	-10.4 (0.2)	2.0 (0.3)	-14 (4)
<i>P. aeruginosa</i>	1.3 (0.1)	-9.8 (0.5)	1.8 (0.3)	-15 (4)

<sup>a</sup>Dipole moments are reported in Debye. <sup>b</sup>Polarizabilities are reported in Å<sup>3</sup>. The standard deviation in the reported values derived from measurements of three to four independent samples are reported in parentheses.

improved as seen by comparison of Figures 4b and 4c. The improvement in the quality of the fit for PA azurin is less significant. (Compare Figures 4f and 4g.) The resulting values of  $|\overline{\Delta\mu}|$  and  $\langle\overline{\Delta\alpha}\rangle$  are compiled in Table 2.

A second method for fitting overlapping spectra, described in the Experimental section, is to deconvolve the absorption band into Gaussians that each represent one of the underlying electronic states. The Gaussians chosen to model the absorption bands of AD and PA azurin are shown in Figures 4a and 4e, respectively, and the parameters defining each are summarized in Table 1. The weak transition at low energy in both the AD and PA absorption spectra corresponds to a  $d-d$  transition and the two higher-energy transitions are both CT in character. Because the  $d-d$  transitions respond weakly to the field, the Gaussians corresponding to these states (Gaussians I and IV) are not included in the fitting. Therefore the fits shown in Figures 4d and 4h represent the results of using only the two dominant CT transitions (Gaussians II and III) to fit the electroabsorption spectra of both proteins. The advantage of this fitting technique over the truncation method described above is that it allows us to obtain high-quality fits for both electroabsorption spectra over a wider wavenumber range (compare Figures 4c with 4d and 4g with 4h, respectively). The extracted molecular parameters are summarized in Table 2.

It is important to point out here that the various fitting methods used yield fairly consistent values of  $|\overline{\Delta\mu}|$  and  $\langle\overline{\Delta\alpha}\rangle$  for the main CT band (Table 2), as would be expected when a single transition dominates a complex absorption band. Specifically, for both azurins, the fits to the truncated absorption spectrum (Figures 4c and 4g) yield values of 1.3–1.4 D for  $|\overline{\Delta\mu}|$ , whereas the fits obtained using Gaussians (Figures 4d and 4h) yielded values of 1.8–2.0 D. Therefore, a primary advantage of using the Gaussian fitting method described above is that it allows us to assess the field response of the weaker electronic transitions, albeit in a semiquantitative fashion. From inspection of the electroabsorption spectra of both azurins, it is evident that both of the CT transitions make the largest contribution to the electroabsorption but the field response of the  $d-d$  transitions is negligible. Indeed, the weaker CT transitions at higher energy exhibit the strongest field response. However, because of the inherent uncertainty in fitting such weak and/or broadly overlapping transitions, the values are not reported here.

One notable feature of the electroabsorption spectra of both azurins is the large *negative* contribution from the *zeroth-derivative* of the absorption spectrum that is required to fit the data obtained at  $\chi = 54.7^\circ$  (see Figures 3c and 3d, dotted curve). The average value of the  $a_{54.7}$  parameter for both azurins derived from the fits shown in Figure 3 is  $\sim -1.5 \times 10^{-16}$  (cm/V)<sup>2</sup>. This value is an order of magnitude smaller than those that have been reported for organic donor–acceptor molecules<sup>37</sup> and similar in magnitude, *although opposite in sign*, to those

observed for inorganic mixed-valence charge-transfer complexes.<sup>16</sup> In the azurins studied here, the relative contribution of the zeroth-derivative term is magnified because their overall field response is small. This term will be discussed in more detail in the Discussion section.

From the standpoint of molecular parameters, two notable results of the electroabsorption studies presented here can be summarized as follows. For the CysS- $\pi$  $\rightarrow$ Cu LMCT band of both AD and PA azurin, a value of  $|\overline{\Delta\mu}|$  of  $\sim 1.3$ –2.0 D is measured, which is significantly smaller than what would be predicted for the transfer of one full electron between the ligand and the metal. The measured value of  $|\overline{\Delta\mu}|$  is compared with the value predicted by electronic structure calculation in the Discussion section. For both azurins, this same CT band exhibits a value of  $\langle\overline{\Delta\alpha}\rangle$  that is *negative* and  $\sim 10$ –20 Å<sup>3</sup> in magnitude. Possible implications of this fairly unusual result are also outlined in the Discussion section.

## Discussion

**Interpretation of  $|\overline{\Delta\mu}|$ .** Similar values for  $|\overline{\Delta\mu}|$  are found for both AD and PA azurin, essentially independent of the fitting method used. Moreover, measurements at two angles of the angle  $\chi$  show that  $\overline{\Delta\mu}$  is nearly parallel to the transition moment for the main charge-transfer transition (ratio of  $\epsilon_{54.7}/\epsilon_{90} \sim 1.67$ , see Experimental section) which lies along the Cu–S bond.<sup>38</sup> In contrast, a value for  $|\overline{\Delta\mu}|$  of  $\sim 10$  D is expected if a full electron charge were to be transferred between the donor and acceptor orbitals with the separation estimated as the crystallographic distance of 2.15 Å.<sup>39</sup> Therefore, it is clear that only partial charge transfer occurs on excitation, in agreement with the results of the semiempirical calculations and X-ray absorption experiments reported.<sup>9,22–27</sup> These earlier studies predict  $\sim 0.2$  e transferred over a maximum of 2.15 Å, yielding an estimate for  $|\overline{\Delta\mu}|$  of  $\sim 2.1$  D, which is in reasonable agreement with the value reported here. However, to compare with a gas-phase calculation, our experimental  $|\overline{\Delta\mu}|$  should be scaled further *downward* by a local field factor that, in proteins, is likely to be slightly larger than 1.<sup>40,41</sup> However, because the local field factor in these systems is not known, no attempt was made to perform this scaling.

In short, our agreement with previous workers is essentially quantitative and provides a good independent measure of the degree of charge transfer associated with the optical transition of this system. The relatively small degree of charge transfer of this transition has been rationalized by the observation that the electron in the ground state is *already* strongly delocalized because of the high degree of covalency of the Cu–S bond.

**Interpretation of  $\langle\overline{\Delta\alpha}\rangle$ .** Because it is unusual to measure a substantial negative value of  $\langle\overline{\Delta\alpha}\rangle$  as we have reported here for both PA and AD azurins, this observation warrants further discussion. It is important to remember that, although  $\overline{\Delta\alpha}$  itself is a tensor quantity, the experiment yields its average value or  $1/3\text{Tr}(\overline{\Delta\alpha})$ . Therefore, it is helpful to make some simplifying assumptions to interpret this result. The first is that the polarizability is highly anisotropic along the Cu–S direction in both the ground and excited states. This in turn implies that the largest diagonal component of  $\overline{\Delta\alpha}$  is predicted to be that lying along the direction defined by  $|\overline{\Delta\mu}|$ . Because therefore we need not explicitly consider changes in the components of the polarizability in the remaining two axes directions, we may directly equate a negative value of  $\langle\overline{\Delta\alpha}\rangle$  with a decrease in polarizability in the excited state. Given that the greatest change in electron density is expected along the Cu–S bond, this assumption is entirely reasonable and is common in the reports

of Stark spectroscopy on MLCT and LMCT states in inorganic complexes. Moreover, one can extract the value of the component of  $\underline{\Delta\alpha}$  parallel to the transition moment (which also lies along the Cu–S bond) by measurements at a second angle of the applied field relative to the direction of polarization of light ( $\chi$ ). Experimentally, we find values of  $\mathbf{b}_{54.7}/\mathbf{b}_{90}$  that are close to 1.67, which indicates that  $\text{Tr}(\underline{\Delta\alpha}) \sim \Delta\alpha_m$  (see Experimental section).

The second simplifying assumption made here is that the contribution of the transition moment polarizability ( $A_{ij}$ ) term in the expression for  $\langle\underline{\Delta\alpha}\rangle$  (the first term in eq 3) may be neglected. Such an assumption seems reasonable on several grounds. Although there is a nonnegligible zeroth-order contribution to the electroabsorption spectrum for both azurins, the corresponding  $\mathbf{a}_\chi$  value derived from the fit of the data at  $\chi = 54.7^\circ$  is *negative*. This implies that the value of  $\mathbf{a}_\chi$  is predominantly due to the contribution of the term proportional to the transition moment hyperpolarizability ( $B_{ij}$ ). This may be concluded because, in principle, this term may be negative, whereas the term proportional to  $A_{ij}$  appears as the square (eq 2). Therefore, the term proportional to  $A_{ij}$  contributes to a lesser extent to the value of  $\mathbf{a}_\chi$  than does that proportional to  $B_{ij}$ . In some cases, symmetry arguments can also be made to derive the same conclusion.<sup>37</sup> Furthermore, the term in eq 3 containing  $A_{ij}$  is multiplied by  $|\Delta\mu|$ , which is also known to be small both based on the measurements presented here and other work.<sup>9,22–27</sup> Finally, within the context of the two-state model (see below), Vance and co-workers have shown that the hyperpolarizability contribution to  $\langle\underline{\Delta\alpha}\rangle$  is given as  $4(|\Delta\mu|)^2/E_{eg}$ , where  $E_{eg}$  is the optical gap of the system.<sup>15</sup> Using this expression<sup>42</sup> yields a value of  $3 \text{ \AA}^3$  with the parameters appropriate for azurin. Again, this represents a relatively small correction to the experimental value of  $\sim -15 \text{ \AA}^3$ .

To explain the negative values of  $\langle\underline{\Delta\alpha}\rangle$  that we have measured for both AD and PA azurins, we adopted the following approach. In the sum-over-states, expression (one-dimensional case) for the polarizability of a state  $i$  in a multilevel system is given as  $\sum_j |\mu_{ij}|^2 / (E_i - E_j)$  in which  $\mu_{ij}$  represents the transition moment between electronic state  $i$  and all other states  $j$ , and  $E$  represents the energy of the respective states. Hence, the polarizability of each state is determined by its transition moment to *all* other electronic states of the system weighted by the inverse of the energy difference between them. This sum usually is dominated by interactions with electronic states higher in energy than those involved in the electronic transition, resulting in a *positive* value for each component of  $\underline{\Delta\alpha}$  due to the effect of the energy denominator. However, for azurins, as for other blue copper proteins, there are several  $d-d$  transitions that lie between the main charge transfer state and the ground state.<sup>6</sup> As evidenced by the weak oscillator strengths of the  $d-d$  bands (see Figure 2), the transition moments between these states and the ground state are small. As a result, they will contribute negligibly to the ground-state polarizability despite the small energy gap involved. In contrast, there is indirect evidence from the literature on plastocyanins that the interaction between at least some of these  $d-d$  states and the charge-transfer excited state may be substantial. If one or more of these  $d-d$  levels also lie at lower energy than the Franck–Condon region of the optically excited state, these could contribute in a negative sense to its polarizability, making the value of  $\langle\underline{\Delta\alpha}\rangle$  negative.

The evidence for a strong coupling between the Franck–Condon and the low-lying  $d-d$  states is that the fluorescence intensities of both azurin and plastocyanin are substantially weaker than would be expected based on the oscillator strength

of the corresponding main charge-transfer absorption bands. Fraga et al.<sup>43</sup> have shown that, for parsley plastocyanin, the optically prepared state decays in roughly 20 fs based on the measurement of a fluorescence quantum yield of  $2.3 \times 10^{-7}$ . Because the ground-state recovery time is on the order of 250 fs, as measured independently by Book et al.<sup>17</sup> and by Edington et al.<sup>18</sup> it can be surmised that the initial relaxation populates one or more of the Cu  $d$  levels before the return of the molecule to the ground state. Unfortunately, to our knowledge, there is no clear signature of a strong absorption between one of the  $d$  levels and the charge-transfer state in the published time-resolved measurements that would lend further support to this picture.

An interesting perspective on this issue is presented in the work of Shin et al.,<sup>13</sup> who measured the Stark spectrum of a series of LMCT and MLCT transitions in small inorganic complexes entrained in solvent glasses. These authors performed electroabsorption spectroscopy on a series of 23 inorganic ruthenium and osmium complexes and compared their results with the predictions of the two-state approximation.<sup>44–46</sup> The two-state approximation says that the sum describing the polarizabilities of the ground and optically excited states can be reduced to only the contributions made by those two states. This analysis gives rise to the following expressions for  $\underline{\Delta\alpha}$ , the excited-state polarizability ( $\alpha_e$ ), and the ground-state polarizability ( $\alpha_g$ ) where, again, only the component of the polarizability parallel to the transition moment is considered. Therefore, each polarizability reported here is effectively the trace of the corresponding tensor with the only nonzero diagonal elements being those parallel to the transition moment.

$$\underline{\Delta\alpha} = -4 \frac{(\mu_{ge})^2}{(E_e - E_g)} \quad (13)$$

$$\alpha_e = -2 \frac{(\mu_{ge})^2}{(E_e - E_g)} \quad (14)$$

$$\alpha_g = 2 \frac{(\mu_{ge})^2}{(E_e - E_g)} \quad (15)$$

Here,  $\mu_{ge}$  represents the transition moment between the ground and excited states, and  $E_g$  and  $E_e$  represent their respective energies. The necessary implication of this model is that  $\underline{\Delta\alpha}$  will *always* be negative (see eq 13), although this was the case in only *one* of the complexes studied in ref 13. Moreover, the model predicts the somewhat unphysical result that the excited-state polarizability is *also* negative (eq 14). Nonetheless, one can say that the value of the polarizability of the charge-transfer state ( $\alpha_e$ ) derived from eq 14 represents the (negative) contribution of the ground state to the expected value of  $\underline{\Delta\alpha}$ , a quantity that is useful in interpreting the results presented here. A calculation based on the spectroscopic parameters of the azurins (the transition moment of AD azurin is  $0.73 \text{ e\AA}$ ,<sup>47</sup> and the absorption maximum in the glasses used here is  $16\,100 \text{ cm}^{-1}$ ) and eq 15 shows that the ground state contributes a value of  $\sim -2.5 \text{ \AA}^3$  to the average polarizability of the charge-transfer states, yielding a predicted  $\langle\underline{\Delta\alpha}\rangle$  of  $-5 \text{ \AA}^3$  (eq 13). To compare with our experiments, the result of eq 13 must be divided by 3 [i.e.,  $\langle\underline{\Delta\alpha}\rangle = 1/3 \text{Tr}(\underline{\Delta\alpha})$ ] because we have reported  $\langle\underline{\Delta\alpha}\rangle$  here.

Realistically, interactions with higher-lying states will contribute in a positive sense to the polarizability of both the ground state and the charge-transfer state. As a result, the value of  $\langle\underline{\Delta\alpha}\rangle$  for the transition is likely to be *increased* (made more positive)

compared with the prediction of the two-state model. Counteracting this effect are the interactions between the charge-transfer state and lower-lying ligand-field states, discussed above, which may again lower the value of  $\langle \Delta\alpha \rangle$ . The interplay between these factors may explain that what we feel is a somewhat fortuitous degree of agreement between our experimental results and the predictions of the two-state model. Nonetheless, these model calculations suggest that interactions between the CT excited state with both the ground state and the low-lying ligand-field states could make an important contribution to the overall value of  $\langle \Delta\alpha \rangle$ .

To illustrate the relationship predicted by the two-state model between  $|\Delta\mu|$  and  $\langle \Delta\alpha \rangle$  and the properties of the electronic wave function of the system, ref 13 contains a graph of the percent mixing of the metal and ligand orbitals versus the values of  $|\Delta\mu|$  and  $\langle \Delta\alpha \rangle$  for an optical charge-transfer transition that would be predicted from the two-state model. A near-zero value for  $|\Delta\mu|$  and the maximum negative value of  $\langle \Delta\alpha \rangle$  are predicted for the complete delocalization of the electron between the metal and ligand orbitals. In this context, our findings of a small value of  $|\Delta\mu|$  and a negative value of  $\langle \Delta\alpha \rangle$  for azurin are therefore *both* consistent with a highly covalent Cu–S bond, as predicted previously<sup>9,22–27</sup>

**Field Effect on the Transition Moment of Azurins.** It was noted earlier that the zeroth-derivative of the absorption spectrum makes a nonnegligible contribution to the fitting of the electroabsorption spectra of PA azurin and to a lesser extent AD azurin, particularly when compared with the first- and second-derivative contributions, which are small. (Figures 3c and 3d). Generally, a large zeroth-order contribution to the electroabsorption spectrum (large  $\mathbf{a}_\chi$  in eq 2), is interpreted to mean that the magnitude of the transition moment is altered by the externally applied field, leading to a change in absorption cross-section. This effect is perhaps not surprising because there are several electronic levels close in energy to the main charge-transfer band in both azurins. Field-induced mixing between these levels could therefore have a measurable effect on the magnitude of the transition moment between the ground and charge-transfer state.

Earlier we argued that, because  $\mathbf{a}_{54.7}$  is negative, its value is determined primarily by the value of the term in  $B_{ijj}$  (eq 2 for  $\chi = 54.7^\circ$ ). Again, the two-state model can be used to predict the value of  $B_{ijj}$  and therefore of  $\mathbf{a}_{54.7}$ , based on the values of the transition moment, ground and excited-state energy gap, and the value of  $|\Delta\mu|$  measured here using eq 16 below.<sup>13</sup>

$$B_{zzz} = \frac{2\mu_{ge}(\Delta\mu)^2 - 4(\mu_{ge})^3}{(E_e - E_g)^2} \quad (16)$$

Here again we make the simplifying assumption that  $B_{zzz}$  is the only nonzero element in the hyperpolarizability tensor. For AD azurin, this analysis yields a *negative* value of  $B_{zzz}$  [ $-3.6 \times 10^{-9} \text{ \AA}^3/(\text{V/cm})$ ], consistent with experimental results. However, the predicted value of  $\mathbf{a}_{54.7}$  is  $\sim 100$  times *smaller* than that measured, indicating that terms in the hyperpolarizability tensor other than  $B_{zzz}$  contribute significantly to the overall field effect on the transition moment in these proteins.

**Electron-Transfer Parameters Derived from Stark Measurements.** The quantities derived for azurin via electroabsorption may be used to estimate two other quantities of interest in predicting electron-transfer rates, namely the electronic matrix element ( $H_{ab}$ ) linking the two diabatic states in the (optical in this case) electron-transfer process and the effective electron-transfer distance ( $R_{ab}$ ) between the two centers. Using the

expression of Cave and Newton (eq 1 in ref 48) for the matrix element and the values of 1.7 D for  $|\Delta\mu|$ , 0.73 eÅ for the transition dipole moment, and 16 100  $\text{cm}^{-1}$  for the energy separation between the two states in AD azurin yields a value of  $\sim 7800 \text{ cm}^{-1}$  for  $H_{ab}$ . This is within the range of what had been estimated for MLCT transitions in several small inorganic complexes.<sup>13,45,48</sup>

For electron-transfer transitions, the value of  $R_{ab}$  is estimated as  $|\Delta\mu|/e$  where  $e$  is the charge on the electron. The values of  $R_{ab}$  that are derived from the experimentally derived values of  $|\Delta\mu|$  for most small inorganic complexes that have been studied to date are significantly *smaller* than the physical separation between the two sites in the electron-transfer process, which is designated as  $R_{ab}^0$ . For AD azurin, assuming again that 0.2e is transferred on excitation and  $|\Delta\mu|$  is 1.7 D,  $R_{ab}$  is calculated to be 1.77 Å. For comparison, the crystallographic value of the separation between the two sites is 2.15 Å.<sup>39</sup> Because the crystallographic data are likely to represent the *maximum* value of  $R_{ab}^0$ , with a more accurate value being that derived from the van der Waals radii of Cu and S, we find fairly good agreement between  $R_{ab}$  and  $R_{ab}^0$ .

#### Solvation Energies Derived from Stark Measurements.

The values of  $|\Delta\mu|$  measured in this experiment also allow us to estimate roughly the response of the environment to optical excitation of the Cu–S center in terms of the predicted Stokes shift between the absorption and emission energies. This result gives insight into the contribution of solvation of the excited state to the ultrafast pump–probe studies of blue copper proteins that have been published to date. Here we estimate the reorganization energy of 300–400  $\text{cm}^{-1}$  based on an estimate of the local dielectric constant as 2 and a comparison with the known solvatochromic dye coumarin 153 (C153).<sup>49</sup> For this estimate, the value of  $|\Delta\mu|$  for C153 was 6 D and that of azurin, 2 D. No attempt was made to account for the expected difference in cavity size between the two systems. The data for the Stokes shift of C153 in various solvents was taken from ref 49. The solvation energy for azurin in an environment with a local dielectric constant of 2 was roughly estimated by calculating one half of the observed Stokes shift between the maxima of the C153 absorption versus emission spectra and scaling this shift in wavenumbers by the ratio of  $|\Delta\mu|^2$  for azurin to that of C153 (i.e.,  $2^2/6^2$ ). By increasing the estimated local dielectric constant to 182 (dimethylformamide), the predicted solvation energy could be as large as 500  $\text{cm}^{-1}$ . These rough estimates are in very good agreement with the value obtained by modeling the absolute Raman cross-sections of plastocyanin using a Brownian oscillator model to estimate the solvation contribution, although they are approximately a factor of 2 lower than those obtained from a similar analysis for azurin. This may reflect the possibility, suggested in ref 32, that the solvation energy of azurin could be overestimated because the population decay caused by fluorescence could not be taken into account. To allow a more quantitative comparison between the electronic properties and predicted solvation behavior of azurin and plastocyanin, experiments are now in progress to measure the values of  $|\Delta\mu|$  and  $\langle \Delta\alpha \rangle$  of the latter system.<sup>28</sup>

#### Conclusions

The values of  $|\Delta\mu|$  and  $\langle \Delta\alpha \rangle$  are reported for the  $\text{Cys}(\text{S},\pi) \rightarrow \text{Cu}(\text{d}_{x^2-y^2})$  LMCT transitions of two azurins, *A. denitrificans* and *P. aeruginosa* as measured by Stark spectroscopy. For both species,  $|\Delta\mu|$  is small ( $\sim 1.3$ – $2.0$  D), in agreement with previous predictions from electronic structure calculations and X-ray absorption experiments. The polariz-

ability of the excited state for the same transition was *smaller* than the ground state by about  $10\text{--}20 \text{ \AA}^3$ . This unusual finding of a negative value for  $\langle \Delta\alpha \rangle$  has been rationalized within the two-state model. Finally, we have also derived a value ( $7800 \text{ cm}^{-1}$ ) for electron-transfer matrix element,  $H_{ab}$ , that is similar in magnitude to those that have been measured for the LMCT transitions of numerous inorganic complexes.

**Acknowledgment.** L. A. P. and A. C. would like to thank Dr. Michael Hendrich and Dr. Hyung Kim for useful discussions. We also acknowledge our sources of funding, The NSF-CAREER and POWRE programs, and the Center for Molecular Analysis at Carnegie Mellon University for the use of the absorption spectrometer. G. R. L. and M. A. W. would like to acknowledge the Microbacterial Growth Facility at the University of Alberta, R. Mah and M. Pickard for growing the *P. aeruginosa* and *A. denitrificans* bacteria, and financial support for this work from the Natural Science and Engineering Research Council (NSERC) of Canada.

## References and Notes

- (1) Adman, E. T. *Adv. Protein Chem.* **1991**, *42*, 145.
- (2) Adman, E. T. In *Metalloproteins-Part 1: Metal Proteins with Redox Roles*; Harrison, P. M., Ed.; Verlag Chemie: Florida, 1985; p 1.
- (3) Sykes, A. G. *Adv. Inorg. Chem.* **1991**, *36*, 377.
- (4) Ainscough, E. W.; Bingham, A. G.; Brodie, A. M.; Ellis, W. R.; Gray, H. B.; Loehr, T. M.; Plowman, J. E.; Norris, G. E.; Baker, E. N. *Biochemistry* **1987**, *26*, 71.
- (5) Solomon, E. I.; Hare, J. W.; Gray, H. B. *Proc. Natl. Acad. Sci. U.S.A.* **1976**, *73*, 1389.
- (6) Solomon, E. I.; Hare, J. W.; Dooley, D. M.; Dawson, J. H.; Stephens, P. J.; Gray, H. B. *J. Am. Chem. Soc.* **1980**, *102*, 168–178.
- (7) Tang, S.-P. W.; Coleman, J. E.; Myer, Y. P. *J. Biol. Chem.* **1968**, *243*, 4286.
- (8) Gewirth, A. A.; Solomon, E. I. *J. Am. Chem. Soc.* **1988**, *110*, 3811.
- (9) Solomon, E. I.; Lowery, M. D. *Science* **1993**, *259*, 1575–1581.
- (10) Di Bilio, A. J.; Chang, T. K.; Malmstrom, B. G.; Gray, H. B.; Karlsson, B. G.; Nordling, M.; Pascjer, T.; Lundberg, L. G. *Inorg. Chim. Acta* **1992**, *145*, 198–200.
- (11) Gray, H. B.; Malmstrom, B. G. *Comments Inorg. Chem.* **1983**, *2*, 203.
- (12) Oh, D. H.; Sano, M.; Boxer, S. G. *J. Am. Chem. Soc.* **1991**, *113*, 6880–6890.
- (13) Shin, Y.-g.; Brunschwig, B. C.; Creutz, C.; Sutin, N. *J. Phys. Chem.* **1996**, *100*, 8157.
- (14) Bubblitz, G. U.; Boxer, S. G. *Annu. Rev. Phys. Chem.* **1997**, *48*, 213–242.
- (15) Vance, F. W.; Karki, L.; Reigle, J. K.; Hupp, J. T.; Ratner, M. J. *Phys. Chem. A* **1998**, *102*, 8320–8324.
- (16) Bubblitz, G. U.; Laidlaw, W. M.; Denning, R. G.; Boxer, S. G. *J. Am. Chem. Soc.* **1998**, *120*, 6068–6075.
- (17) Book, L. D.; Arnett, D. C.; Hu, H.; Scherer, N. F. *J. Phys. Chem. A* **1998**, *102*, 4350–4359.
- (18) Edington, M. D.; Diffey, W. M.; Doria, W. J.; Riter, R. E.; Beck, W. F. *Chem. Phys. Lett.* **1997**, *275*, 119–126.
- (19) Ungar, L. W.; Scherer, N. F.; Voth, G. A. *Biophys. J.* **1997**, *72*, 5–17.
- (20) Pierce, D. W.; Boxer, S. G. *Biophys. J.* **1995**, *68*, 1583–1591.
- (21) Premvardhan, L. L.; Peteanu, L. A. *J. Phys. Chem. A* **1999**, *103*, 7506–7514.
- (22) Penfield, K. W.; Gewirth, A. A.; Solomon, E. I. *J. Am. Chem. Soc.* **1985**, *107*, 4519–4529.
- (23) Larsson, S.; Broo, A.; Sjölin, L. *J. Phys. Chem.* **1995**, *99*, 4860–4865.
- (24) Pierloot, K.; De Kerpel, J. O. A.; Ryde, U.; Olsson, M. H. M.; Roos, B. O. *J. Am. Chem. Soc.* **1998**, *120*, 13156–13166.
- (25) Pierloot, K.; De Kerpel, J. O. A.; Ryde, U.; Roos, B. O. *J. Am. Chem. Soc.* **1997**, *119*, 218–226.
- (26) George, S. J.; Lowery, M. D.; Solomon, E. I.; Cramer, S. P. *J. Am. Chem. Soc.* **1993**, *115*, 2968–2969.
- (27) Shadle, S. E.; Penner-Hahn, J. E.; Schugar, H. J.; Hedman, B.; Hodgson, K. O.; Solomon, E. I. *J. Am. Chem. Soc.* **1993**, *115*, 767–776.
- (28) Chowdhury, A.; Peteanu, L. A.; Fraga, E.; Loppnow, G. R. Manuscript in preparation.
- (29) St. Clair, C. S.; Ellis, W. R. J.; Gray, H. B. *Inorg. Chim. Acta* **1992**, *191*, 149.
- (30) Ambler, R. P. *Biochem. J.* **1963**, *89*, 341.
- (31) Ambler, R. P.; Wynn, M. *Biochem. J.* **1973**, *131*, 485.
- (32) Webb, M. A.; Kwong, C. M.; Loppnow, G. R. *J. Phys. Chem. B* **1997**, *101*, 5062–5069.
- (33) Abraham, Z. H. L.; Lowe, D. J.; Smith, B. E. *Biochem. J.* **1993**, *295*, 587.
- (34) Dodd, F. E.; Hasnain, S. S.; Hunter, W. N.; Abraham, Z. H. L.; Debenham, M.; Kanzler, H.; Eldridge, M.; Eady, R. R.; Ambler, R. P.; Smith, B. E. *Biochemistry* **1995**, *34*, 10180.
- (35) Liptay, W. Dipole Moments and Polarizabilities of Molecules in Excited Electronic States. In *Excited States*; Lim, E. C., Ed.; Academic Press: New York, 1974; pp 129–229.
- (36) The centers of the Gaussians (Table 1) used for PA azurin are in very good agreement with those obtained by Solomon and co-workers.<sup>6</sup> However, the widths of the Gaussians reported here are narrower than those in ref 6 because the absorption spectrum that we obtain of PA azurin in 50% glycerol-buffer glass (pH 8.8) at 77 K is narrower than that of the protein in a film shown in ref 6. In the course of the fitting, we obtained two separate sets of Gaussians that gave very good fits to the 77 K absorption spectrum. However, these were rejected because they did not agree with the published MCD data. Nevertheless, the  $|\Delta\mu|$  and  $\langle \Delta\alpha \rangle$  values obtained from fitting the electroabsorption signal using any of these three different sets of Gaussians lie within the limits of experimental error.
- (37) Bubblitz, G. U.; Ortiz, R.; Marder, S. R.; Boxer, S. G. *J. Am. Chem. Soc.* **1997**, *119*, 3365–3376.
- (38) The error margins on these measurements, which are due to the weakness of the Stark signal and the complexity of the fitting required (see below), suggest that the maximum angle between  $\bar{m}$  and  $\Delta\mu$  is  $\sim 20^\circ$ .
- (39) Baker, E. N. *J. Mol. Biol.* **1988**, *203*, 1071.
- (40) Gottfried, D. S.; Steffen, M. A.; Boxer, S. G. *Science* **1991**, *251*, 662–665.
- (41) Franzen, S.; Boxer, S. G. *J. Phys. Chem.* **1993**, *97*, 6304.
- (42) Our equations differ slightly from those of ref 15 because we report the average value of  $\Delta\alpha$  rather than its trace.
- (43) Fraga, E.; Webb, M. A.; Loppnow, G. R. *J. Phys. Chem.* **1996**, *100*, 3278–3287.
- (44) Oudar, J. L. *J. Chem. Phys.* **1977**, *67*, 446.
- (45) Creutz, C.; Newton, M. D.; Sutin, N. *J. Photochem. Photobiol. A Chem.* **1994**, *82*, 47–59.
- (46) Reimers, J. R.; Hush, N. S. *J. Phys. Chem.* **1991**, *95*, 9773–9781.
- (47) Webb, M. A.; Loppnow, G. R. *J. Phys. Chem. B* **1998**, *102*, 8923–8929.
- (48) Cave, R. J.; Newton, M. D. *Chem. Phys. Lett.* **1996**, *249*, 15–19.
- (49) Horng, M. L.; Gardecki, J. A.; Papazyan, A.; Maroncelli, M. *J. Phys. Chem.* **1995**, *99*, 17311–17337.